42–50 Nucleic Acids Research, 1995, Vol. 23, No. 1

Stability of adriamycin-induced DNA adducts and interstrand crosslinks

Anne van Rosmalen, Carleen Cullinane, Suzanne M. Cutts and Don R. Phillips*

School of Biochemistry, La Trobe University, Bundoora, Victoria 3083, Australia

Received October 18, 1994; Revised and Accepted December 1, 1994

ABSTRACT

The stability of adriamycin-induced DNA adducts and interstrand crosslinks was measured at 37°C by three independent procedures. The loss of [^{14}C]-labelled adducts was described by two first-order decays with half-lives of 7.4 h (60% amplitude) and 39 h (40%). The loss of the drug chromophore also exhibited a biphasic character, with half-lives of 6 h (65%) and ~150 h (35%). The decay of transcriptional blockages at an isolated, apparent interstrand GpC crosslinking site was described by two first-order processes, with half-lives of 3 h (65%) and 40 h (35%), whereas the decay of transcriptional blockages at an isolated guanine residue (apparent site of monoadduct) was completely described by a first-order decay with a half-life of 5.3 h. The loss of interstrand crosslinks was measured using a gel electrophoresis assay, and the decay was characterised by a single first-order process with a half-life of 4.7 h. Collectively, these values serve to define a model of the interstrand crosslink with unstable sites of attachment at both ends of the crosslink, with half-lives at either end being ~5 and 40 h. The adducts exhibited increasing lability with increasing pH, and were particularly unstable at pH 12, with a half-life of ~0.5 h. The adducts were also heat labile, with an overall melting temperature of 67°C (10 min exposure) and this was also the thermal lability measured at three individual adduct sites probed by λ exonuclease.

INTRODUCTION

The anthracycline antibiotic adriamycin has been the single most successful agent used in cancer chemotherapy since its discovery almost 25 years ago [1]. In contrast to other anticancer agents, adriamycin displays high clinical activity against a broad spectrum of tumours [2] and has been a particularly successful agent in the treatment of breast cancer [3]. Despite the clinical utility of adriamycin, its use is limited primarily by its dose-related cardiotoxicity and myelosuppression [4], together with the development of drug resistance [5].

In an effort to develop a rational design for derivatives of adriamycin with increased efficacy and fewer limiting side effects, there has been an intense study of the mechanism of antitumour activity of this drug. Despite this intensive research effort, the mode of action of adriamycin still remains unclear [6]. A large body of evidence, however, suggests that the major action of the drug is mediated through its effects on DNA [1,6]. Indeed, a microfluorescence technique has demonstrated that in cells treated with adriamycin >99% of the drug detected in the nucleus is associated with DNA [7]. At the DNA level two mechanisms have been proposed: one involves impairment of topoisomerase II activity, while the other involves reductive activation of the drug [6,8].

Adriamycin is readily reduced by numerous cellular flavoproteins including xanthine oxidase and NADH dehydrogenase [9–11]. One-electron reduction of adriamycin under aerobic conditions yields a semiquinone radical which rapidly transfers an electron to molecular O_2, initiating a cascade of reactions which manifest in the formation of the powerful oxidant, the hydroxyl radical [12,13]. Such radicals have been implicated both in the cardiotoxicity of adriamycin [14] and in its mode of antitumour action [15].

Two-electron reduction of adriamycin under anaerobic conditions has been proposed to generate a DNA alkylating intermediate, the quinone methide [16]. These anthracycline quinone methides have been shown to react with both electrophiles [17,18] and nucleophiles [19–21], including the nucleic acid component 2′-deoxyguanosine [22].

The formation of DNA adducts following microsomal activation of adriamycin was first reported by Sinha and Chignell [23]. Since this initial report numerous studies have detected the formation of adriamycin-induced DNA adducts *in vitro* [24,25], in cell culture [26] and *in vivo* [27,28]. Adriamycin-induced interstrand crosslinks have also been detected *in vitro* [29] and in drug-treated cells in culture [30]. We have also utilised an *in vitro* transcription assay to detect the slow formation of adriamycin-induced blockages to RNA polymerase at GpC sequences, consistent with the presence of adriamycin adducts [31], and have used several crosslinking assays to demonstrate the same time-dependent formation of DNA interstrand crosslinks [29]. The crosslinks therefore appear to form at GpC sequences, and are also formed by enzymatic reduction with xanthine oxidase [32].

Given the extensive evidence for the formation of adriamycin-induced adducts and interstrand crosslinks, both *in vitro* and *in vivo*, and the possibility that these lesions may contribute to the mode of action of the drug, it is surprising that the chemical nature

* To whom correspondence should be addressed

of these complexes has not yet been established [29]. The reason for this delay in obtaining structural information of these complexes is largely because they are only partially stable. Both the adducts and interstrand crosslinks formed *in vitro* are heat labile [32], as are adducts formed with cyanomorpholinoadriamycin [33]. The interstrand crosslinks formed in cell culture studies are also known to be heat and alkali labile [30,34]. Since the most definitive description of the structures of these complexes is likely to come from 3D-NMR studies of oligonucleotide–drug adducts and crosslinks, it is critical to have a thorough understanding of the stability of these complexes prior to attempting such experiments. We therefore present here a quantitative examination of the stability of these adducts and interstrand crosslinks *in vitro*, and show that a significant amount of these complexes exhibit a half life of ~40 h at 37°C.

MATERIALS AND METHODS

Materials

[14-^{14}C]Adriamycin (55 μCi/mmol) was purchased from Amersham (UK). Adriamycin was a gift from Farmitalia Carlo Erba (Milan). Molecular biology grade phenol was obtained from IBI (CT), and λ exonuclease was from Bethesda Research Laboratories (MD). The Klenow fragment of *E.coli* DNA polymerase I was from Pharmacia (WI) and the Nensorb 20 columns were purchased from NEN Research Products (DE).

DNA source

Calf thymus DNA was purchased from Worthington Biochemical Corporation (NJ). The plasmid SP64 was grown in *E.coli* JM101 cells and harvested using the routine alkaline lysis method [35]. The plasmid was digested with *Eco*RI and the 5′-overhang filled in using the Klenow fragment of *E.coli* DNA polymerase I and [α-^{32}P]dATP. The labelled fragment was purified as described previously by chromatography through a Nensorb 20 column [29] and resuspended in sonicated calf thymus DNA in TE buffer to yield a final concentration of 300 μM bp of labelled fragment.

The 186 bp *Eco*RI–*Pvu*II fragment was isolated from pCC1 and 3′-end-labelled as described previously [33]. For transcript studies, the 497 bp fragment (containing the lac UV5 promoter) was isolated from pRW1 as described elsewhere [36].

λ exonuclease detection of adriamycin adducts

25 μM bp of the end-labelled 186 bp fragment was reacted with 5 μM adriamycin and 10 μM Fe(III) for 24 h to form adriamycin adducts. At the completion of the reaction the unbound drug was removed by phenol/chloroform extraction and the DNA precipitated and then resuspended in reaction buffer (40 mM Tris, pH 8.0, 100 mM KCl, 3 mM $MgCl_2$ and 0.1 mM EDTA). Aliquots (10 μl) were removed and subjected to a 10 min incubation at temperatures between 50 and 90°C. Aliquots (2.5 μl) of each of the heat-treated samples were then reacted with 2 U of λ exonuclease in buffer containing 67 mM glycine–KOH, pH 9.4, 2.5 mM $MgCl_2$ and 50 μg/ml BSA. The reaction was incubated at 37°C for 60 min, after which an equal volume of formamide loading dye (90% formamide, 10 mM EDTA, 0.1% xylene cyanol and 0.1% bromophenol blue) was added to terminate the reaction. The samples were subsequently denatured and subjected to extended electrophoresis through an 8% polyacrylamide gel. The gel was subsequently fixed, dried and autoradiographed using standard procedures [36]. Quantitation was performed using a 400B PhosphorImager and ImageQuant software (Molecular Dynamics, CA).

Stability of adriamycin adducts

Method A: [^{14}C]adriamycin. 25 μM bp pSP64/*Pvu*II DNA was reacted for 48 h with 10 μM [^{14}C]adriamycin and 40 μM Fe(III) ions in reaction buffer (pH 8) and 7 mM DTT. Unbound drug was removed by phenol/chloroform extraction [29,32], the DNA precipitated and resuspended in reaction buffer. The adriamycin adduct-containing fragment was further incubated at 37°C for various times up to 96 h, after which any released drug was removed by a final phenol extraction. The amount of non-extractable drug remaining bound to the DNA was determined by scintillation counting on a Wallac 1410 scintillation counter.

Method B: absorbance of adducts. Calf thymus DNA (500 ml, 25 μM bp) was reacted for 48 h with 10 μM adriamycin, 10 μM Fe(III) and 2 mM DTT in reaction buffer to form maximal levels of DNA–adriamycin adducts. Unbound drug was removed by phenol/chloroform extraction, the DNA precipitated and resuspended in 5 ml of reaction buffer. The absorbance of adducts was determined spectrophotometrically at 508 nm. The adducts were further incubated at 37°C for time periods up to 90 h. Aliquots (500 μl) were taken at time intervals and released drug was removed by a final phenol extraction. The amount of non-extractable drug remaining bound to the DNA was then measured again at 508 nm.

For detection of the thermal stability of adducts, the adducts were formed with calf thymus DNA and purified by phenol extraction as described above. The adducts were then heated for 10 min at temperatures from 50 to 90°C, then subjected to additional phenol/chloroform extractions prior to measurement of the residual absorbance at 508 nm.

Stability of interstrand crosslinks at 37°C

25 μM end-labelled *Eco*RI-digested pSP64 DNA was reacted for 5 h with 10 μM adriamycin and 10 μM Fe(III) to form sub-maximal levels of DNA interstrand crosslinks. Unbound drug was removed by phenol/chloroform extraction and the DNA was subsequently ethanol precipitated and resuspended in reaction buffer. The crosslinked DNA was further incubated with an additional 5 μM Fe(III) ions at 37°C for periods up to 24 h. Aliquots were removed, ethanol precipitated and then resuspended in 0.2× TE. A denaturing loading buffer (60% DMSO, 1 mM EDTA, 0.04% xylene cyanol and 0.04% bromophenol blue) was added to yield a final concentration of 35% DMSO and the samples were denatured at 60°C for 5 min prior to electrophoresis through a 0.8% agarose gel overnight [29]. The gel was dried, autoradiographed and subsequently quantitated using a 400B PhosphorImager and ImageQuant software (Molecular Dynamics, CA).

In vitro transcription

The 497 bp DNA fragment (25 μM) was incubated for 36 h in the presence of 10 μM adriamycin and 40 μM Fe(III). The DNA was subsequently ethanol precipitated and resuspended in reaction buffer. Transcription initiation and elongation from the lac UV5

promoter was performed as described previously [36]. Transcription was terminated at defined time periods up to 48 h by removing 5 µl aliquots of the transcription mix and adding to 5 µl of loading termination buffer. Samples were denatured for 5 min at 90°C prior to loading on a 12% polyacrylamide gel. Autoradiography and analysis were performed as described above.

pH stability of adriamycin adducts

Adriamycin adducts were prepared with calf thymus DNA as described above, but in a reaction buffer adjusted to pH 6, 7, 8 or 12. After phenol/chloroform extractions and ethanol precipitation the pellets were resuspended in reaction buffer at the appropriate pH and the absorbance measured at 508 nm at time intervals on standing at 37°C. Extraction of released adducts was as described above.

Thermal denaturation

Adriamycin adducts were prepared with calf thymus DNA as described above and redissolved in the reaction buffer. The DNA concentration was adjusted to yield an absorbance at 260 nm of 0.5–1.0 and 250 µl then degassed with helium for 10 min. Denaturation of the DNA was carried out using a Gilford Model 2527 Thermoprogrammer attached to a Gilford 240 spectrophotometer, using a heating rate of 0.5°C/min.

Estimation of half-lives

The half-life of loss of adduct or crosslinks was obtained from a first-order analysis of the decay of these quantities. Where the decay was not fully described by one exponential, the slower process was first evaluated from the limiting slope at long decay times, and the second decay determined in a similar manner from the residual contribution after 'peeling' from the slower exponential decay. All dissociation rate constants were obtained from the least squares estimation of the fit, with the standard deviation of the slope, providing an estimate of the error of the rate constant (and hence of the half-life).

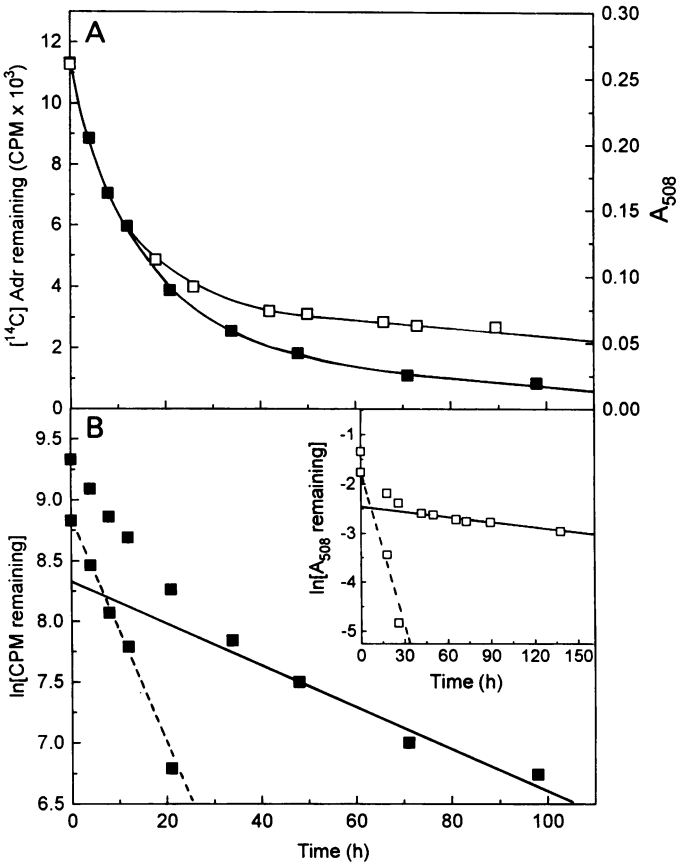

Figure 1. Loss of adriamycin-induced adducts at 37°C. DNA was reacted at pH 8 with 10 µM [^{14}C]adriamycin (■) or adriamycin (□) for 48 h in the presence of 10 µM Fe(III) ions, with phenol/chloroform extraction, ethanol precipitation and then resuspended in reaction buffer. The DNA–adduct complex was then re-incubated at 37°C for up to 96 h and residual adducts quantitated by scintillation counting of [^{14}C] or by absorbance of the drug chromophore at 508 nm (**A**). A first order analysis of the decay of adducts is shown in (**B**), where the continuous line represents the slow dissociation process and the dashed line the faster dissociation process ('peeled' data points) associated with the loss of [^{14}C] labelled drug (■). The same first order analysis of the loss of drug chromophore is shown in the inset (□).

RESULTS

Stability of adducts at 37°C

It has been known for some years that adriamycin-induced adducts formed *in vitro* are unstable to some degree [30]. In order to have an understanding of the extent of this instability, the adduct decay profile was measured at 37°C. For this purpose, linearised pSP64 was reacted with [^{14}C] adriamycin to form high levels of DNA adducts and unreacted and non-bound drug was removed by phenol/chloroform extraction. The purified adduct-containing fragment was then incubated at 37°C for an extended period and lability of the adduct measured as a loss of radioactivity from the fragment following a further phenol extraction. A profile of decay of adducts is shown in Figure 1A. The loss of adducts was resolved into two first-order kinetic processes (Figure 1B). The half-life of the slowly dissociating species was 39 ± 6 h (from the least squares fit of the limiting slope from 34–96 h), with the contribution of this process 'peeled' from the faster dissociating process. The half-life of the rapidly dissociating process was 7.4 ± 0.3 h and comprised 60% of the total amplitude of the dissociating species.

The lability of the adriamycin adducts at 37°C was confirmed independently by directly measuring the time-dependent release of the drug chromophore from a purified DNA fragment containing adriamycin adducts. As seen in Figure 1A, the initial release of the drug chromophore as a function of incubation time closely followed that of the release of the radiolabel. The subsequent decay (40–140 h) was somewhat slower, with a half-life of ~150 ± 50 h (Figure 1B), comprising 35% of the total absorbance loss. The half-life of the faster process was ~6 ± 1 h.

The stability of adducts was also examined following exposure to buffers (37°C) from pH 6–12. The stability of the adducts decreased with increasing pH (Figure 2), with relative half lives of ~40, 20, 10 and 0.5 h at pH 6, 7, 8 and 12 respectively (assuming only one decay process at each pH). Since the objective was to establish the overall dependence of the stability of adducts with pH, only a few time points were sampled at each pH, and this precluded a more detailed two exponential analysis as applied to the data shown in Figure 1. If the adduct was not initially purified by phenol extraction, there was no loss with time of exposure to pH 8 (data not shown).

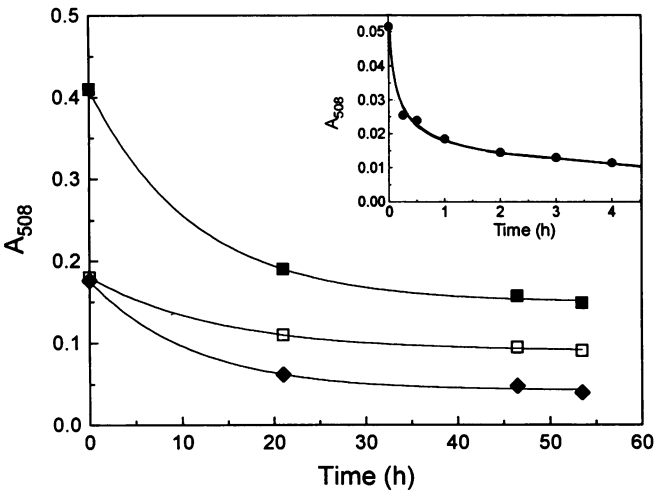

Figure 2. pH stability of adriamycin-induced adducts. DNA was reacted with 10 μM adriamycin and 10 μM Fe(III) ions for 48 h, 37°C in a reaction buffer adjusted to pH 6 (□), 7 (■), 8 (◆) or 12 (●, inset). After phenol/chloroform extractions and ethanol precipitation, the DNA was resuspended in reaction buffer at the same pH as used for formation of the adducts and then incubated at 37°C. At time intervals, the DNA was extracted with phenol/chloroform and adducts quantitated as residual absorbance of drug chromophore at 508 nm.

Thermal stability of adducts

Lambda exonuclease was used to probe the thermal stability adducts at individual sites. A 186 bp DNA fragment was reacted with adriamycin to form adducts, and unreacted drug was subsequently extracted with phenol/chloroform to eliminate the possibility of any thermal stability of the adducts arising from the presence of intercalated drug. The fragment was exposed to high temperature for 10 min, after which the DNA was digested with λ exonuclease, a 5′→3′ exonuclease, and the presence of adducts was detected as sequence-specific blockages to enzyme digestion. The resolved digestion products are shown in Figure 3A.

The control DNA fragments were fully digested by the enzyme, as evidenced by the lack of radioactivity associated with the control lanes. Enzyme digestion of the drug-reacted template however was inhibited at several sites throughout the template with each of these drug-induced blockage regions staggered over several nucleotides. The drug-induced inhibition of the unheated (20°C) template was quantitated and the sequence specificity of the blockages is presented in Figure 3B. Ten isolated blockage regions were evident on the region of the template resolved. All of these sites were associated with one or more 5′-GpC sequences on the DNA template, confirming the previously established specificity of adriamycin adducts for such sequences on duplex DNA [31]. Every 5′-GpC sequence present on the template was associated with inhibition of the exonuclease. At each isolated 5′-GpC sequence the blockage consisted of a 2–3 base staggered block reducing in intensity to within 0–2 bases of the 5′-GpC sequence. The staggered enzyme digestion observed is not an adriamycin-dependent phenomenon, but rather a general characteristic of λ exonuclease detection of any drug bound to DNA, as observed previously with *cis*-DDP, anthramycin and mitomycin C [37].

The thermal lability of each of the adriamycin adduct sites is evident from the decreasing amount of radioactivity associated with each drug blockage site as a function of increasing temperature to which the DNA adduct was exposed (Figure 3A). The temperature-dependent loss of the drug-induced enzyme blockages at each of the first three drug sites encountered by λ exonuclease (sites 1–3) was quantitated and is expressed in Figure 3C as a percentage of the initial blockage detected in the 20°C lane at that site. Only the initial three blockage sites were quantitated, because at low temperatures (e.g. 20°C) the amount of enzyme reaching later drug sites is low due to the enzyme progression being blocked at earlier drug sites, hence the intensity of drug blockage at these later sites is underestimated. At higher temperatures however, the loss of drug-induced blockages enables more exonuclease to reach the later drug sites, leading to a relative overestimation of the intensity of the blockages at these later drug blockage sites.

Each of the three sites quantitated demonstrated thermal lability over a narrow temperature range. The average mid-point melting temperature for these three sites was ~67°C.

The thermal lability was also monitored from the residual absorbance of adducts at 508 nm. The mid-point melting temperature for the loss of chromophore was 70°C by this procedure.

Lifetime of transcriptional blockages

An *in vitro* transcription assay was employed to examine the stability of adducts at individual adduct sites. Adducts were formed on a DNA fragment containing the lac UV5 promoter. The initiated complex was then formed with *E.coli* RNA polymerase and elongation of the entire sample was commenced by the addition of high concentrations of all four ribonucleotides. This solution was sampled at time intervals and the resulting transcripts visualised by high resolution gel electrophoresis and autoradiography (Figure 4A). The major blockage sites detected were all at GpC sequences, as observed previously [31]. Most of the transcriptional blockages decayed with increasing elongation time.

The intensity of the first major blocked transcript (position 37, with the blockage corresponding to G of the 5′-AGCT non-template sequence) was quantitated and subjected to a first-order kinetic analysis (Figure 4B). The slower dissociating process is characterised by a half-life of 40 ± 5 h and accounted for 35% of the amplitude of the blockage, while the faster process exhibited a half-life of 3 ± 1 h. Blockage at position 60, prior to the first isolated guanine residue at position 61 (flanked by an A.T bp on either side) was also subjected to a first order kinetic analysis, and revealed a single dissociation process with a half-life of 5.3 ± 0.7 h (Figure 4B).

Thermal denaturation

To test the possibility that the adducts might arise merely from thermal stabilisation of the DNA, the melting profile of drug-treated DNA was measured and compared to untreated DNA (Figure 5). No detectable thermal stabilisation was induced by the adducts, since both the control DNA and DNA–adduct complex exhibited the same melting temperature of 87°C at 260 nm. However, when the DNA denaturation was monitored at 508 nm, the drug chromophore exhibited an apparent melting temperature of 94°C, with a hyperchromicity of 30%, consistent with release of the adduct from the DNA. There was essentially no release of adduct until at least 50% denaturation of the DNA.

Stability of crosslinks

End-labelled linear SP64 DNA was reacted with adriamycin to form a sub-maximal level of DNA interstrand crosslinks. Unreacted and intercalated drug were removed by phenol/chloroform extractions. The drug-treated DNA was then incubated at 37°C and the extent of crosslinking remaining sampled at intervals up to 24 h. Crosslinking was determined by denaturing the DNA in 35% DMSO at 60°C for 5 min. Under these conditions unreacted dsDNA denatures and migrates as ssDNA. In contrast, much of the drug-treated DNA migrates as the duplex form following these denaturing conditions (Figure 6A, zero incubation time at 37°C). The extent of crosslinking decreased with increasing incubation time at 37°C. This time-dependent loss of crosslinking was quantitated and analysed in terms of a first-order decay process. The decay was completely described by a first-order process with a half-life of 4.7 ± 0.7 h (Figure 6B).

DISCUSSION

Heat lability of adducts and crosslinks

The sequence specificity observed upon digestion of the adriamycin-treated DNA template with λ exonuclease provides independent verification of the exclusive specificity of adriamycin for 5′-GC sequences, with all enzyme blockages associated with such sequences. The ability of λ exonuclease to detect adriamycin adducts provided a convenient means by which to measure the thermal stability of these individual drug blockage sites. The increased ability of the enzyme to digest past all of the drug-induced blockage sites following heat treatment implies that the adduct itself was heat labile. Previous studies utilising [^{14}C] adriamycin to measure the overall loss of adducts from a 3000 bp DNA fragment revealed an adduct melting temperature of 70°C, similar to that observed here at individual adduct sites. Since the radiolabelled drug assay directly measures the release of the drug

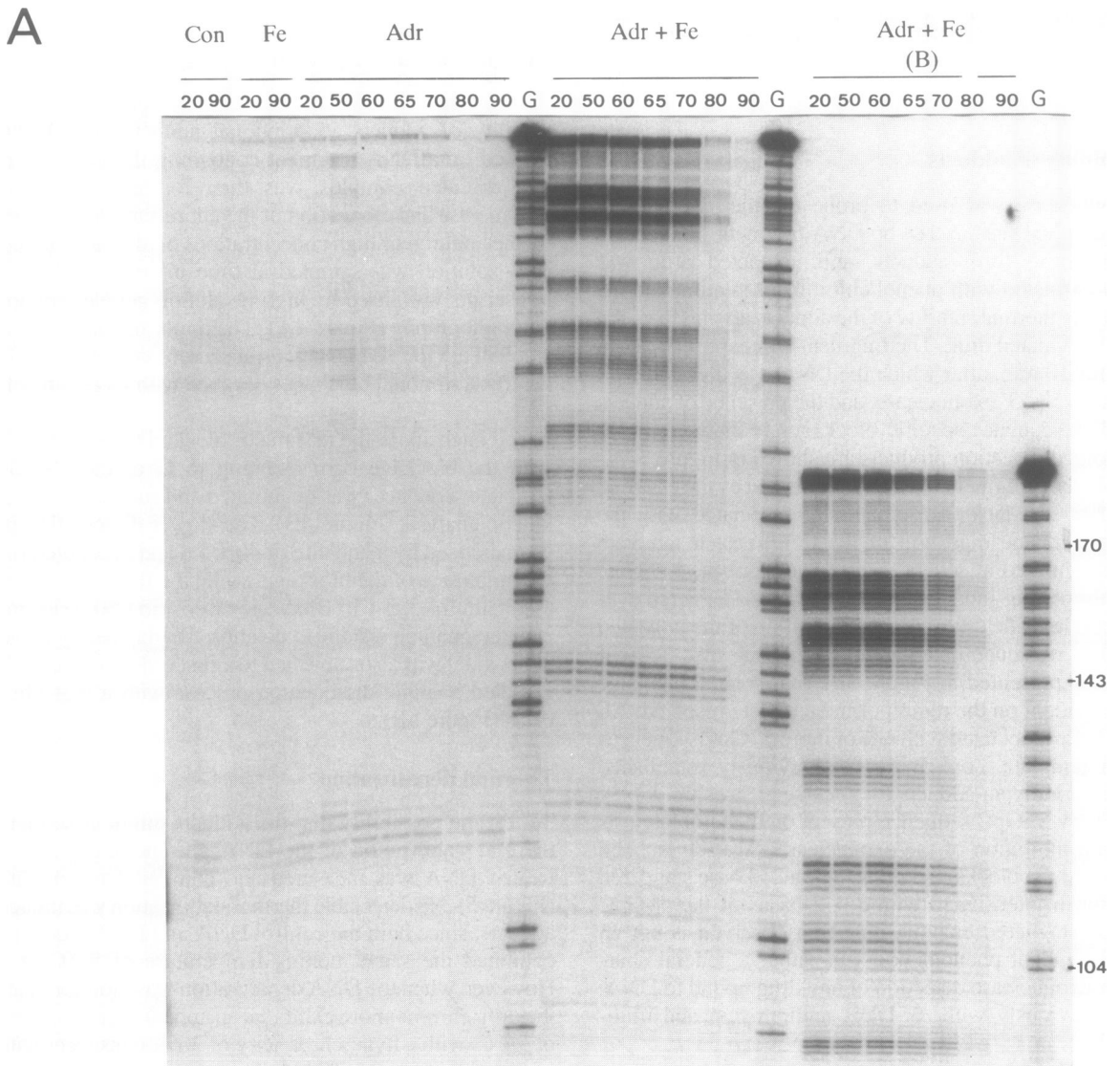

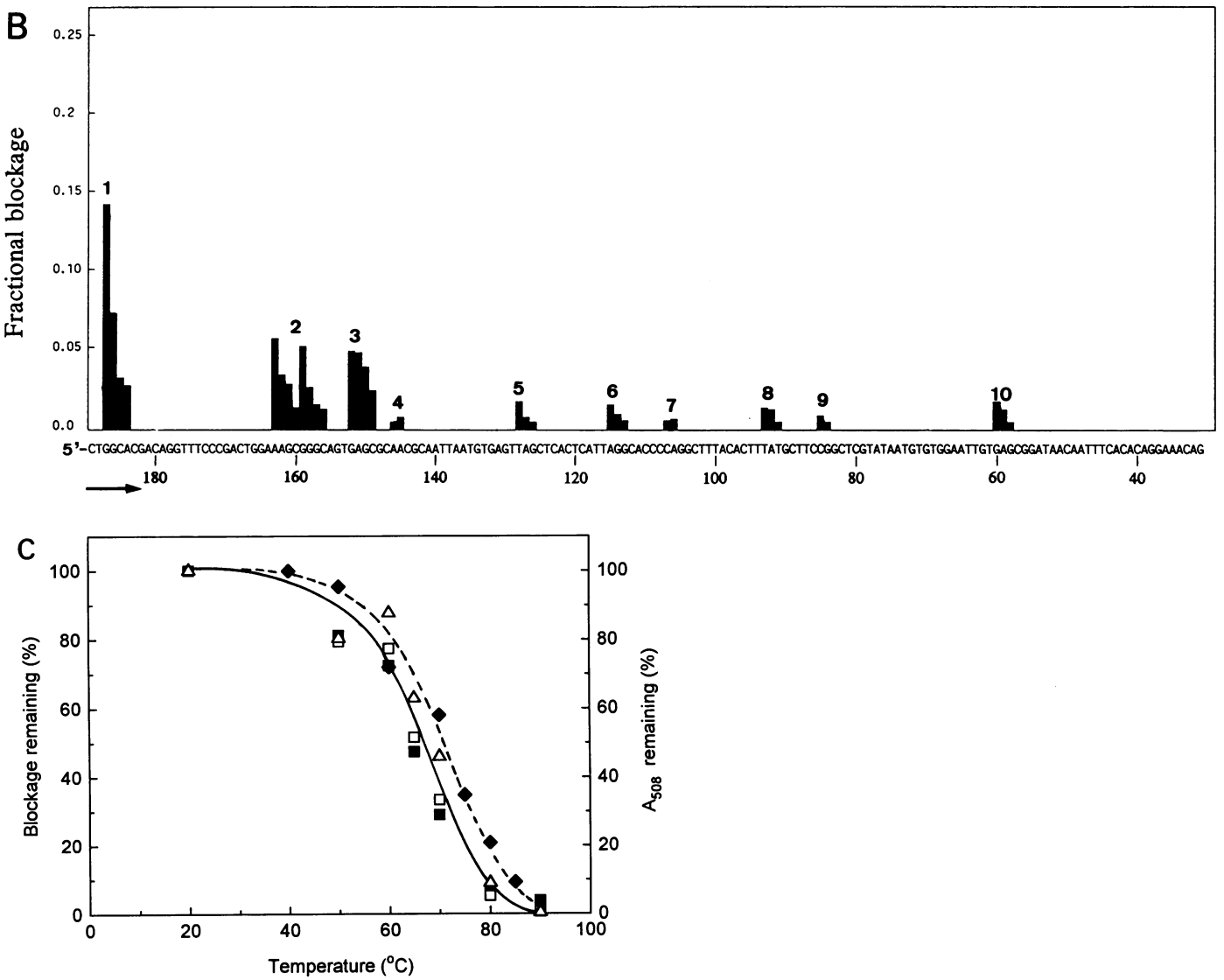

Figure 3. λ exonuclease detection of adriamycin-induced adducts. An end-labelled 186 bp DNA fragment was incubated for 24 h in the presence of 5 μM adriamycin (Adr), 10 μM Fe(III) ions (Fe) or both adriamycin and Fe(III) ions (Adr + Fe) prior to phenol/chloroform extraction, ethanol precipitation and resuspension in reaction buffer. A control was performed in which the DNA was incubated in the absence of both adriamycin and Fe(III) ions. Aliquots were exposed to increasing temperatures (20–90°C) for 10 min before digestion of the DNA with λ exonuclease and separation of the products on an 8% denaturing polyacrylamide gel. (**A**) Autoradiogram of λ exonuclease digests. Lane G represents a Maxam–Gilbert G sequencing lane. The right hand eight lanes (denoted B) were subjected to twice the electrophoresis time of the other lanes. The location of the blockage sites is shown as the length of DNA relative to the 3′-labelled end of the DNA. The length of some DNA fragments is shown on the extreme right. (**B**) Sequence specificity of adriamycin-induced adducts. The fraction of DNA molecules blocked from the λ exonuclease digestion was determined from the 20°C lane of the adriamycin/Fe(III)-treated DNA of (A). The direction of enzyme digestion is shown by the arrow and numbering is relative to the 3′-labelled end of the DNA. The blockage sites are numbered sequentially as encountered by λ exonuclease from the 5′-end of the labelled strand. (**C**) Thermal stability of individual blockage sites. The extent of blockage of λ exonuclease is shown for sites 1 (■), 2 (□) and 3 (△) of (B), relative to the amount of blockage experienced at the same site at 20°C (continuous line). The relative amount of total adduct (measured as the drug chromophore at 508 nm) remaining after a 10 min exposure to increasing temperatures (◆) is shown as a dashed line.

from the DNA, the similarity in the melting temperatures therefore implies that the temperature-dependent loss of blockages observed in the λ exonuclease assay is indeed due to the release of adduct from the DNA. This has also been confirmed by the melting profiles, where the chromophore of the adduct exhibits a 30% hyperchromicity only after almost complete loss of secondary structure of the DNA. The hyperchromicity presumably reflects the release of drug from a DNA-bound state and suggests that the chromophore of the adduct probably exists in some type of intercalated state. The further implication is that even though the sites of attachment of drug to DNA are labile, the 'liberated' chromophore remains associated with the DNA, and can only be removed by vigorous procedures such as extraction with phenol (as in Figure 3C) or by complete destruction of the DNA secondary structure at high temperature (as in Figure 5). The initial decrease of absorbance of the chromophore at 50–80°C (Figure 5) is likely to be due to slight stereochemical rearrangement of the adduct accompanying increased flexibility of the DNA duplex at higher temperatures.

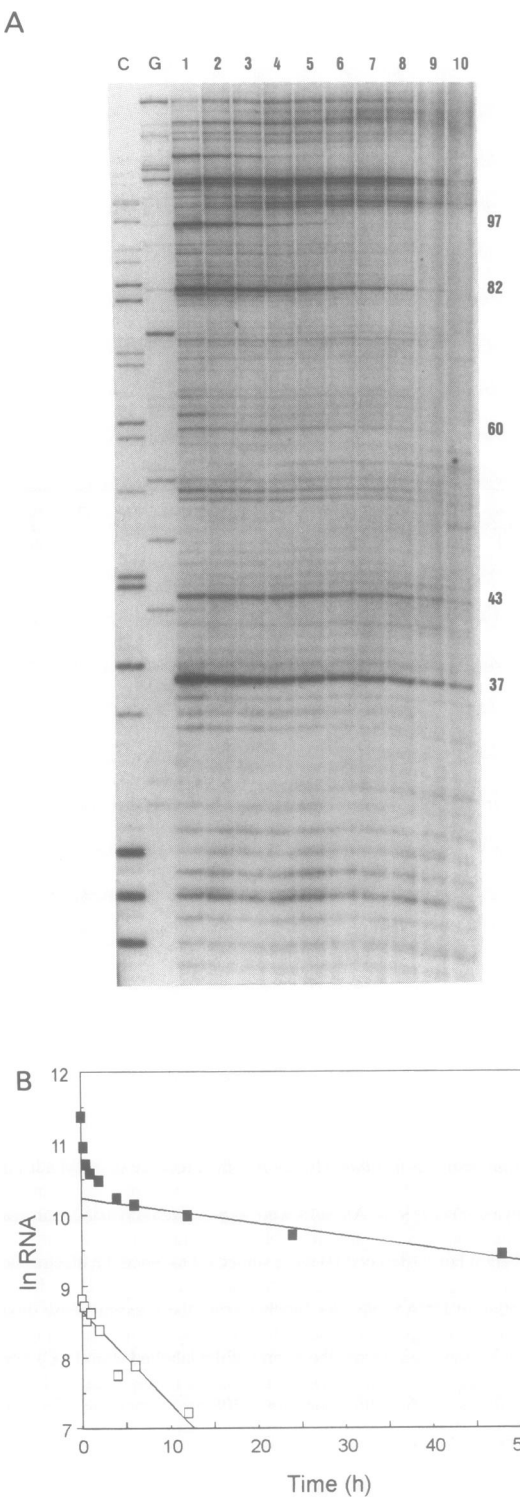

Figure 4. Elongation of the transcription complex past adriamycin-induced blockage sites. (**A**) Adriamycin (10 μM) was reacted with the 497 bp fragment containing the lac UV5 promoter. Subsequent elongation of the initiated transcription complex was allowed to proceed for 1, 15 or 30 min or 1, 2, 4, 6, 12, 24 or 48 h (lanes 1–10). C and G denote sequencing lanes terminated by the inclusion of 3′-*O*-methoxy CTP and 3′-*O*-methoxy GTP, respectively. The numbering represents the length of the RNA transcript beginning with G of the initiating GpA dinucleotide [31]. (**B**) The amount of RNA transcript at the 37mer (■) and 61mer (□) blockage sites were quantitated by phosphorimager analysis and subjected to first-order kinetic analysis.

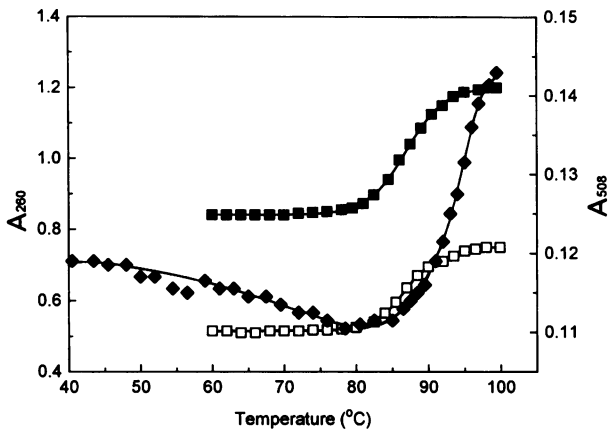

Figure 5. Denaturation of DNA–adduct complexes. Adriamycin-induced adducts and crosslinks were formed, purified by phenol/chloroform extraction and ethanol precipitation and resuspended in reaction buffer. DNA denaturation was monitored at 260 nm (■) and release of drug at 508 nm (◆). Untreated DNA (i.e. not exposed to adriamycin) was also monitored at 260 nm (□).

Alkali lability

The extreme lability of the interstrand crosslink at pH 12 may well account for the lack of detection of such crosslinks by alkali elution. This technique is carried out at pH 12 over long time periods, and it is now apparent that under these conditions most of the crosslinks would have been destroyed. In contrast, procedures which have avoided extended times of exposure to high pH in the DNA isolation and crosslink analysis procedure have detected crosslinks both *in vitro* [29] and *in vivo* [39].

Model of decay of adducts and crosslinks at 37°C

The instability of adriamycin-induced adducts and crosslinks was not confined to the effects at high temperatures. Loss of both adducts and crosslinks also occurred at a physiological temperature and these decays were quantitated by several procedures which reflect the average amount of adducts and crosslinks remaining with time, as well as by a transcription assay which yields the decay parameters at individual guanine and GpC sites. The half-lives of these processes have been summarised in Table 1 and collectively enable a model to be developed which accounts for all of the observed dissociation processes.

The basis of this model is that adducts form at only two sites: GpC sequences (the major site) and isolated guanine residues, where the occupancy was only ~10% of that at individual GpC sites [31]. Since the half-life of adducts at isolated guanine residues is ~5.3 h at 37°C, then this can be assumed (as a first approximation) to be similar to that for the site of attachment to guanine at one end of the interstrand crosslink at GpC sequences. If this is the case there are two important conclusions. Firstly, the half-life of the second arm of attachment in the interstrand GpC crosslink is ~40 h, since this is the only other decay rate observed for the loss of adducts from the GpC site. Secondly, since the more labile end of the crosslink has an expected half-life of 5.3 h, then the half-life of the crosslink itself would be predicted to be ~5.3 h. Since this value is in good agreement with the experimental determination of the half-life of the crosslink itself (4.7 h) this provides a good deal of confidence in this model.

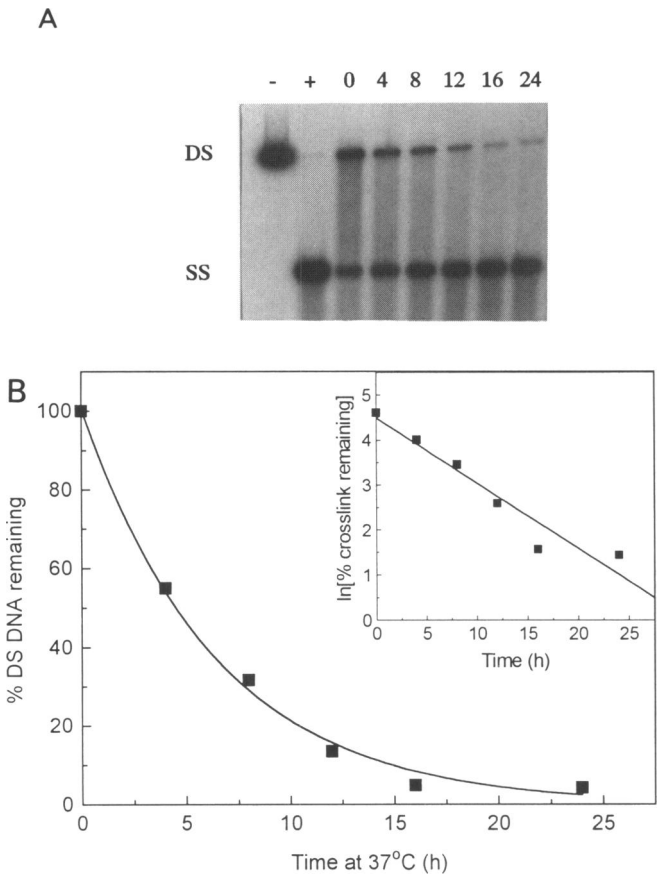

Figure 6. Stability of adriamycin-induced DNA interstrand crosslinks at 37°C. (**A**) End-labelled pSP64/*Eco*RI DNA was reacted with 10 μM adriamycin and 10 μM Fe(III) ions for 5 h prior to purification of the crosslinked DNA by phenol/chloroform extraction and ethanol precipitation. The DNA was resuspended in reaction buffer with 5 μM Fe(III) ions and incubated at 37°C for up to 24 h. At time intervals, aliquots were removed and the DNA precipitated and resuspended in 0.2× TE. A DMSO loading buffer was added and the samples denatured and electrophoresed through 0.8% agarose overnight. Unheated control DNA is denoted as (–) and denatured control DNA as (+). Double-strand DNA is denoted as DS and single-strand DNA as SS. (**B**) Decay of adriamycin-induced DNA interstrand crosslinks at 37°C. The relative amount of adriamycin-induced crosslinked DNA is shown at increasing times relative to the amount at zero time after resuspension in reaction buffer at 37°C. The inset shows the first-order kinetic analysis of the decay of crosslinks.

There are several further implications of this model. Since the half-life of the longer-lived component of crosslinks at an individual GpC site is 40 h (Figure 4B), then the average value for decay from all the GpC interstrand crosslinks would be expected to be of a similar value. This is indeed the case; the experimental value for loss of radioactively labelled adduct was essentially identical (39 h). The value of ~150 ± 50 h (measured using large scale preparation of adduct, and quantitating the loss of adducts by residual absorbance of the chromophore) is subject to a large error which arises from the small absorbance changes measured in the 40–140 h time range, and therefore is not as reliable as the radiolabelled-derived data. Nevertheless, it is quite clear that a significant fraction of the adducts (35–40%) are long lived, with a half-life of the order of 40–150 h.

Table 1. Half-lives of decay of adriamycin-induced adducts and interstrand crosslinks at 37°C

Type of decay	$t_{1/2}$ (h) fast	slow
All adducts[a] (^{14}C)		
(absorbance)	7.4 ± 0.3 (60%)	39 ± 6 (40%)
	6 ± 1 (65%)	150 ± 50 (35%)
Isolated G[b]	5.3 ± 0.7 (100%)	
GpC[c]	3[e] ± 1 (65%)	40 ± 5 (35%)[f]
Crosslink[d]	4.7 ± 0.7 (100%)	

[a]Calculated from decay of radiolabelled drug or loss of absorbance (Figure 1).
[b]Calculated from the decay of blocked transcripts at site 60 (Figure 4A) and quantitated in Figure 4B.
[c]Calculated from the decay of blocked transcripts at site 37 (Figure 4A) and quantitated in Figure 4B.
[d]Calculated from the decay of crosslinking (Figure 6A) and quantitated in Figure 6B.
[e]Calculated from the 0–3 h decay of blocked transcripts published previously (site 37 of Figure 7 in reference 33).
[f]The amplitude of the slow decay was calculated from Figure 4B.

The shorter half-life of 7.4 h observed for the loss of radiolabelled adducts presumably reflects the average of contributions from isolated guanine residues (5.3 h), together with the loss of adducts from interstrand crosslinks where one end of the crosslink has already been broken.

There are two possible reasons why adducts appear to be completely stable if not purified by phenol extraction. Either the purification procedure itself removes a stabilising component of these complexes or (more likely) removal of the excess unreacted drug shifts the equilibrium to a unidirectional dissociation process. It is therefore likely that the adducts may well be considerably more stable in a cellular environment. It also suggests that future structural studies of the adducts and crosslinks would be best performed with the non-purified complexes if this is possible.

Biological significance

High levels of Fe^{3+} were employed in this study in order to maximise the amount of adduct and crosslink formed. It is therefore relevant to note that in the absence of added Fe^{3+} (residual levels will be present in buffers) both products are still formed, but to a lesser extent [29,31]. The adducts and crosslinks are therefore not artefacts of the presence of high levels of Fe^{3+}.

Although the Fe^{3+} ion-catalysed formation of adriamycin-induced adducts and interstrand crosslinks have now been extensively documented *in vitro* [29,31,32], and a mechanism for this reductive activation has been proposed [29], it is yet to be established if this Fe^{3+} mediated process occurs *in vivo*. The biological source of Fe^{3+} *in vivo* is possibly ferretin, since it has been shown that adriamycin is able to sequester Fe^{3+} from ferretin [40,41]. However, it is more likely that the reductive process is carried out by $1e^-$ or $2e^-$ enzymatic catalysis *in vivo*. Since adriamycin is localised dominantly in the nucleus [7], and the activated species has a half-life of 15 s [17], bioreductive activation is therefore likely to be restricted dominantly to the nucleus. It is significant then that several bioreductive enzymes,

for which adriamycin is a substrate, have been identified in the nucleus (e.g. NADH cytochrome P450 reductase and xanthine oxidase) [8,11,42].

CONCLUSIONS

The adducts and interstrand crosslinks were completely abolished after short exposure to high temperature. The interstrand crosslinks were also extremely unstable at high pH, but both adducts and interstrand crosslinks exhibited modest stability at 37°C. The similarity of these characteristics with the known temperature and alkaline lability of interstrand crosslinks formed in drug-treated cells suggests that the interstrand crosslink detected in both situations (i.e. *in vitro* and in cells) are likely to be the same, or at least similar.

Since there is a good correlation between the capacity of adriamycin derivatives to form interstrand crosslinks and their cytotoxic activity [39], this highlights the need to gain a detailed understanding of the chemistry and biochemistry of these crosslinks. It is likely that new insight into the chemical nature of these crosslinks is likely to come from mass spectral and NMR studies of such crosslinks formed with oligonucleotides. Now that the stability of these adducts and crosslinks are known, this provides an opportunity for these physico-chemical studies of adriamycin-induced adducts and crosslinks with oligonucleotides to proceed. The life-time of the complexes may have to be extended for these studies and this can most readily be accomplished by decreasing the temperature of the complex appropriately.

ACKNOWLEDGEMENTS

This work was carried out with the support of the Australian Research Council (D. R. P.), the Anticancer Council of Victoria (D. R. P.) and Macfarlane Burnet (C. C.) and John Maynard Haedstrom (S. M. C.) postgraduate scholarships. We also thank Farmitalia Carlo Erba for the supply of adriamycin.

REFERENCES

1 Weiss, R.B. (1992) *Semin. Oncol.* **19**, 670–786.
2 DeVita, V.T. Jr., Hellman, S. and Rosenberg, S.A. (1993) *Cancer Principles and Practice of Oncology*, 4th Edn. J.B. Lippincott Company, PA, Vols 1 and 2.
3 Jones, S.E. (1982) *Current Concepts in the Use of Doxorubicin Chemotherapy*. Farmitalia Carlo Erba S.p.A., Milan, Italy.
4 Dorr, R.T. and Jones, S.E. (1982) *Current Concepts in the Use of Doxorubicin Chemotherapy*, (Jones, S.E., ed.). Farmitalia Carlo Erba S.p.A., Milan, Italy, pp 145–154.
5 Nielsen, D. and Skovsgaard, T. (1992) *Biochim. Biophys. Acta* **1139**, 169–183.
6 Myers, C.E., Mimnaugh, E.G., Yeh, G.C. and Sinha, B.K. (1988) *Anthracycline and Anthracenedione-Based Anticancer Agents* (Lown, J.W., ed). Elsevier, Amsterdam, The Netherlands, pp. 527–569.
7 Gigli, M., Doglia, S.M., Millot, J.M., Valentini, L. and Manfait, M. (1988) *Biochim. Biophys. Acta* **950**, 13–20.
8 Cummings, J., Anderson, L., Willmott, N. and Smyth, J.F. (1991) *Eur. J. Cancer* **27**, 532–535.
9 Pan, S-S. and Bachur, N.R. (1980) *Mol. Pharmacol.* **17**, 95–99.
10 Favaudon, V. (1982) *Biochimie* **64**, 457–475.
11 Kappus, H. (1986) *Biochem. Pharmacol.* **35**, 1–6.
12 Land, E.J, Mukherjee, T., Swallow, A.J. and Bruce, J.M. (1983) *Arch. Biochem. Biophys.* **225**, 116–121.
13 Butler, J. and Hoey, B.M. (1987) *Br. J. Cancer* **55**, suppl. VIII, 53–59.
14 Fu, L.X., Waagstein, F. and Hjalmarson, A. (1990) *Int. J. Cardiol.* **29**, 15–20.
15 Sinha, B.K., Katki, A.G., Batist, G., Cowan, K.H. and Myers, C.E. (1987) *Biochemistry* **26**, 3776–3781.
16 Moore, H.W. (1977) *Science* **197**, 527–532.
17 Kleyer, D.L. and Koch, T.H. (1983) *J. Am. Chem. Soc.* **105**, 5154–5155.
18 Fisher, J., Abdella, B.R.J. and McLane, K.E. (1985) *Biochemistry* **24**, 3562–3571.
19 Ramakrishnan, K. and Fisher, J. (1983) *J. Am. Chem. Soc.* **105**, 7187–7188.
20 Ramakrishnan, K. and Fisher, J. (1986) *J. Med. Chem.* **29**, 1215–1221.
21 Gaudiano, G., Friegerio, M., Bravo, P. and Koch, T. (1990) *J. Am. Chem. Soc.* **112**, 6704–6709.
22 Egholm, M. and Koch, T.H. (1989) *J. Am. Chem. Soc.* **111**, 8291–8293.
23 Sinha, B.K. and Chignell, C.F. (1979) *Chemico-Biol. Interact.* **28**, 301–308.
24 Sinha, B.K. (1980) *Chemico-Biol. Interact.* **30**, 66–77.
25 Sinha, B.K. and Gregory, J.L. (1981) *Biochem. Pharmacol.* **30**, 2626–2629.
26 Cummings, J., Bartoszek, A. and Smyth, J.F. (1991) *Analyt. Biochem.* **194**, 146–155.
27 Sinha, B.K. and Sik, R.H. (1980) *Biochem. Pharmacol.* **29**, 1867–1868.
28 Cummings, J., Wilmott, N., Hoey, B.M., Marley, E.S. and Smyth, J.F. (1992) *Biochem. Pharmacol.* **44**, 2165–2174.
29 Cullinane, C., van Rosmalen, A. and Phillips, D.R. (1994) *Biochemistry* **33**, 4632–4638.
30 Konopa, J. (1983) *Biochem. Biophys. Res. Commun.* **110**, 819–826.
31 Cullinane, C. and Phillips, D.R. (1990) *Biochemistry* **29**, 5638–5646.
32 Cullinane, C., Cutts, S.M., van Rosmalen, A. and Phillips, D.R. (1994) *Nucleic Acids Res.* **22**, 2296–2303.
33 Cullinane, C. and Phillips, D.R. (1993) *Nucleic Acids Res.* **21**, 1857–1862.
34 Konopa, J. (1990) *Pharmacol. Ther.* **7** (suppl), 83–94.
35 Sambrook, J., Fritsch, E.F. and Maniatis, T. (1989) *Molecular Cloning. A Laboratory Manual*, 2nd edn. Cold Spring Harbor Laboratory Press, Cold Spring Harbor, NY.
36 Skorobogaty, A., White, R.J., Phillips, D.R. and Reiss, J.A. (1988) *Drug Design Delivery* **3**, 125–152.
37 Mattes, W.B. (1990) *Nucleic Acids Res.* **18**, 3723–3730.
38 Skladanowski, A. and Konopa, J. (1994) *Biochem. Pharmacol.* **47**, 2269–2278.
39 Skladanowski, A. and Konopa, J. (1994) *Biochem. Pharmacol.* **47**, 2279–2287.
40 Demant, E.J., Jr. (1984) *FEBS Lett.* **176**, 97–100.
41 Winterbourn, C.C., Vile, G.F. and Monteiro, H.P. (1991) *Free Radicical Res. Commun.* **1**, 107–114.
42 Sinha, B.K., Trush, M.A., Kennedy, K.A. and Mimnaugh, E.G. (1984) *Cancer Res.* **44**, 2892–2896.